NACA RM L53H21

NACA

RESEARCH MEMORANDUM

INVESTIGATION OF REYNOLDS NUMBER EFFECTS FOR A SERIES

OF CONE-CYLINDER BODIES AT MACH NUMBERS

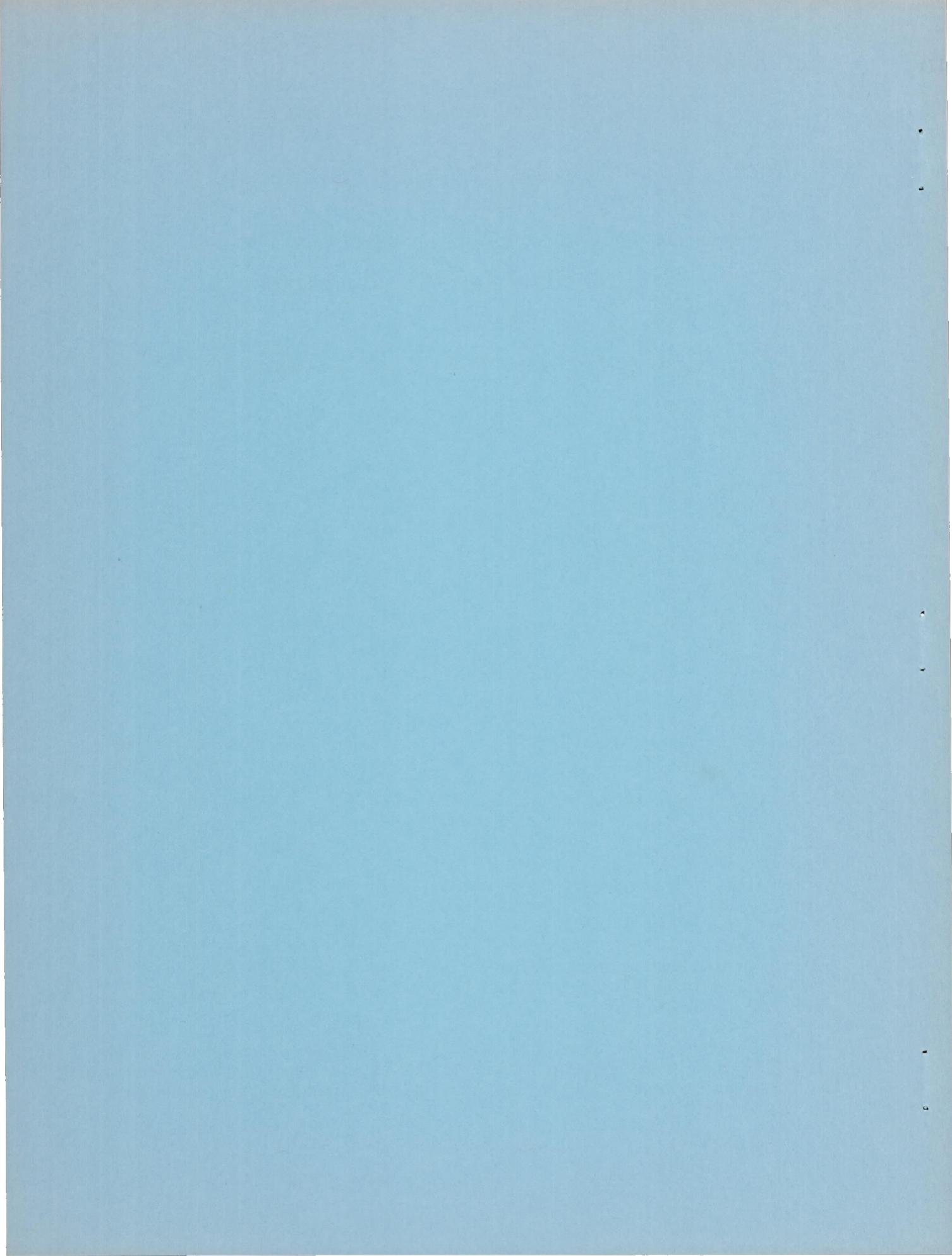OF 1.62, 1.93, AND 2.41

By Carl E. Grigsby and Edmund L. Ogburn

Langley Aeronautical Laboratory
Langley Field, Va.

NATIONAL ADVISORY COMMITTEE
FOR AERONAUTICS

WASHINGTON

October 7, 1953
Declassified August 17, 1955

NATIONAL ADVISORY COMMITTEE FOR AERONAUTICS

———————

RESEARCH MEMORANDUM

———————

INVESTIGATION OF REYNOLDS NUMBER EFFECTS FOR A SERIES

OF CONE-CYLINDER BODIES AT MACH NUMBERS

OF 1.62, 1.93, AND 2.41

By Carl E. Grigsby and Edmund L. Ogburn

SUMMARY

An investigation of the Reynolds number for transition and the skin-friction drag at zero lift of eight cone-cylinder bodies having various fineness ratios has been made at Mach numbers of 1.62, 1.93, and 2.41 over a Reynolds number range from 0.3×10^6 to 10×10^6. The accuracy of the skin-friction data was not sufficient to permit any general conclusions to be drawn. The Reynolds number for transition was found to be dependent upon both the tunnel stagnation pressure and Mach number.

INTRODUCTION

Considerable interest is shown currently in the aerodynamic characteristics of bodies of revolution at supersonic speeds and special attention is shown to the Reynolds number for transition and to the effects of Reynolds number upon the skin-friction drag. In references 1 and 2 results are presented of an investigation of the friction drag and boundary-layer transition on cone-cylinder bodies over a range of Mach number. In this investigation, variations in Reynolds number were made by lengthening the cylindrical portion of the bodies. References 3 to 6 have also presented a considerable amount of aerodynamic data on a series of bodies having near-parabolic and conical noses and cylindrical afterbodies. In these tests, variations in Reynolds number were accomplished by changes in tunnel stagnation pressure. These investigations illustrate two techniques for obtaining the effect of Reynolds number upon skin friction.

In reference 3 data are presented which indicate a dependence of the Reynolds number for transition upon stagnation pressure. It was suggested that changes in tunnel turbulence level were responsible for this effect.

Additional data for bodies of revolution indicating this same phenomenon have been published in references 2 and 6 with results for several hollow cylinders presented in reference 7. Although the temperature was held nearly constant for the wind-tunnel tests, it was not clear that similar results could not have been obtained by variations in temperature, in which case the results would be more properly expressed as a function of Reynolds number per unit length. The need for further research on this phenomenon is apparent.

The purpose of the present investigation was to determine the effects of Mach number and stagnation pressure upon the Reynolds number for transition, and to obtain the zero-lift skin-friction drag from measurements of total drag, base drag, and forebody pressure drag for a series of eight cone-cylinder models of varying fineness ratio. Some objections have been raised about the use of cone-cylinder bodies for skin-friction investigations because of the severe adverse pressure gradient and the possibility of local separation at the juncture of the cone and the cylinder. These objections are based on the belief that this local separation or the adverse pressure gradient or both would make the results of questionable value in assessing theoretical predictions. Although there is some justification for objections on this basis, there is also sufficient reason to investigate these bodies in that they are employed in several current and proposed missiles and have the advantage of simplified construction.

The tests were conducted at Mach numbers of 1.62, 1.93, and 2.41 over a Reynolds number range from about 0.3×10^6 to 10×10^6 for the condition of zero heat transfer.

SYMBOLS

A_{max} maximum cross-sectional area of body (equal to A_B)

A_W wetted area of body (surface area forward of base)

A_B base area

C_{D_T} total-drag coefficient, $\dfrac{\text{Total drag}}{q A_{max}}$

C_{D_B} base-drag coefficient, $P_B \dfrac{A_B}{A_{max}} = P_B$

C_{D_P} forebody pressure-drag coefficient, $\displaystyle\int_0^L P \frac{d}{dx}\left(\frac{r}{r_{max}}\right)^2 dx$

C_f skin-friction coefficient, $\displaystyle\frac{A_B}{A_W}\left[C_{D_T} - \left(C_{D_P} + C_{D_B}\right)\right]$

L body length

r local body radius

r_{max} maximum body radius

P pressure coefficient, $\dfrac{p_l - p_s}{q}$

P_B base pressure coefficient

P_0 stagnation pressure

p_s free-stream static pressure

p_l local static pressure

q free-stream dynamic pressure

M free-stream Mach number

R Reynolds number

R_L free-stream Reynolds number based on model length

R_T transition Reynolds number based on axial length to transition point

T_0 stagnation temperature

APPARATUS AND TESTS

Wind Tunnel

The Langley 9-inch supersonic tunnel is a continuous-operation, closed-circuit type of wind tunnel in which the pressure, temperature, and humidity of the enclosed air can be regulated. Different test Mach numbers are provided by interchangeable nozzle blocks which form test sections approximately 9 inches square. Eleven fine-mesh turbulence-damping screens are installed in the relatively large-area settling chamber ahead of the supersonic nozzle. The turbulence level of the tunnel is considered low, based on the turbulence-level measurements presented in reference 8. A schlieren optical system is provided for qualitative-flow observations.

Models

A sketch illustrating the models and sting support and giving the pertinent dimensions is shown in figure 1, and a photograph of the models is shown in figure 2. The eight models varied in fineness ratio in increments of 1.0 from 2.0 to 9.0. All models for the force tests were made of magnesium and were available from the investigation of reference 9. The surface roughness of these models was about 14 rms microinches. At the beginning of each run the model was polished with a metal polish and carefully wiped with chamois to preserve a uniformity of surface conditions during the tests. The hollow sting which served as a conduit for the strain-gage wires was sealed at the support end and vented to the chamber within the model. The pressure in the hollow sting was measured and was assumed to be the average pressure in the chamber within the model.

A special model constructed of steel having a surface roughness of 8 rms microinches, and otherwise identical with model 8, was employed for the detailed schlieren observations of transition and for the pressure-distribution tests. Pressure orifices were located in the conical nose on the 0°, 90°, 180°, and 270° meridian planes. As in the other models, the hollow sting served as a conduit for the pressure tubes and was sealed at the support end.

The tests were conducted at Mach numbers of 1.62, 1.93, and 2.41 and over a Reynolds number range from about 0.3×10^6 to 10×10^6. The stagnation temperature was $100^\circ \pm 5^\circ F$ and data were obtained only for equilibrium temperature conditions. Throughout the tests the dewpoint was kept sufficiently low to insure negligible effects of condensation. A condition of zero pitch and yaw was maintained as closely as possible.

The first phase of the investigation consisted of detailed schlieren observations of the boundary layer for the visual determination of transition Reynolds numbers of model 8 (steel). This model was later used to measure the pressure distribution over the conical portion of the body. The effect of the tunnel static-pressure distribution upon the forebody pressure drag was found to be negligible.

The second phase of the investigation comprised the measurements of total drag and base drag over the Reynolds number range at each test Mach number. The magnesium models were used for these tests. It will be noted from figure 1 that the strain-gage balance protruded from the rear of models 1 and 2 and caused an interference in the base-pressure measurements. Additional base-pressure measurements were made without the balance, and the total drag measurements were corrected by the difference in the two base-pressure measurements. Additional unknown tare forces may still exist on models 1 and 2; however, these forces are believed to be small, especially for model 2.

Precision of Data

All models were maintained within ±0.15° of zero pitch and yaw with respect to the tunnel sidewalls and center line, respectively. Previous measurements of the flow angularity in the tunnel test section have shown negligible deviations. The extimated accuracies of the test variables and measured coefficients are given in the subsequent table. Values are given for a tunnel stagnation pressure of 30 in. Hg. The accuracies of the coefficients are functions of the stagnation pressure and increase with decreasing stagnation pressure.

Mach number, M . . . . ±0.01

Reynolds number, R, per in. . . . . ±0.004 × 10^6

Total-drag coefficient, C_{D_T} . . . . ±0.003

Forebody pressure-drag coefficient, C_{D_P} . . . . ±0.002

Base-drag coefficient, C_{D_B} . . . . ±0.002

RESULTS AND DISCUSSION

Total and Base Drag

The total-drag coefficients for all models are shown for varying Reynolds number at M = 2.41 in figure 3. These data are typical of the results obtained at the other test Mach numbers. The corresponding base-drag coefficients are shown in figure 4. For model 8, the reflected

nose shock entered the wake at a position such that the base drag was affected (see ref. 10). The variation of both the base- and total-drag coefficients with Reynolds number is typical of the variation shown in previous results for this type of configuration. The effects of both model fineness ratio and Mach number upon base pressure for these configurations have been discussed in reference 9.

Forebody Pressure Drag

Typical pressure distributions over the conical portion of model 8 at $M = 2.41$ are shown in figure 5. These distributions at each Reynolds number were integrated to obtain the forebody pressure-drag coefficients shown in figure 6. It can be seen that the forebody pressure drag is relatively independent of Reynolds number at the Mach numbers tested. The experimental results are also compared with the values from the tables of solutions to the theory of Taylor and Maccoll given in reference 11. The experimental results are about 6 percent higher than theoretical results at $M = 1.62$, in good agreement at $M = 1.93$ and about 4 percent lower at $M = 2.41$.

Skin-Friction Coefficient

The skin-friction data results left much to be desired with regard to accuracy and scatter of the results; consequently, only typical results at $M = 2.41$ will be presented. The skin-friction coefficients were obtained in the following manner:

$$C_f = \frac{A_B}{A_W}\left[C_{D_T} - \left(C_{D_P} + C_{D_B}\right)\right] \tag{1}$$

The results at $M = 2.41$ are shown in figure 7. Also shown in figure 7 are the following theoretical results for laminar flow: the flat-plate incompressible result of Blasius, the compressible result of Chapman and Rubesin, and the flat-plate values corrected to the cone-cylinder by the formula given in reference 2.

$$C_f = C_{f_{\text{flat plate}}}\left[\frac{2}{\sqrt{3}} \frac{\sqrt{(s + a)(s + 3a)}}{s + 2a}\right] \tag{2}$$

where s is the slant height of the cone and a is the length of the
cylindrical afterbody. This formula follows from the transformation by
Mangler and does not consider changes in pressure along the body. The
incompressible, turbulent, skin-friction coefficient is also presented
together with the extended Frankl and Voishel theory. These theoretical
predictions for turbulent flow are presented only as a matter of refer-
ence since there are no comparable experimental results.

The experimental results can be seen to exhibit considerable scatter,
particularly in the transition range where the values of skin-friction
coefficient are smallest. No general conclusion can be drawn from the
results about the effects of varying model fineness ratio upon skin
friction.

Reynolds Number for Transition

From theoretical considerations, it is well known that, for airfoils
at subsonic speeds, the Reynolds number for transition is a function of
wing Reynolds number. This dependency upon wing Reynolds number is a
consequence of the favorable pressure gradient existing over the forward
position of the airfoil. Configurations having zero pressure gradient,
such as flat plates, have transition Reynolds numbers which are invariant
with wing Reynolds numbers. Thus, it is surprising when the results in
reference 7 for hollow cylinders at supersonic speeds show transition
Reynolds numbers which increase with increasing stagnation pressure
(increasing stream Reynolds number). Since, for a given Mach number,
Reynolds number is a function of temperature and pressure, it was not
clear that similar results could not have been obtained by variations
in stagnation temperature in which case the transition Reynolds numbers
would have been shown as a function of Reynolds number per unit length.
However, unpublished data of the transition Reynolds number on a 10° cone
from the Langley 9-inch supersonic tunnel have indicated that decreasing
the stagnation temperature (increasing stream Reynolds number) gave
slightly lower transition Reynolds numbers, whereas increasing the stag-
nation pressure (increasing stream Reynolds number) gave higher transi-
tion Reynolds numbers. Thus, it appears that the effect cannot be iso-
lated as a function of Reynolds number per unit length, but is a function
of some parameter which is influenced by changes in stagnation pressure.

Schlieren photographs of model 8 (steel) were obtained for several
stagnation pressures at each Mach number; typical results at M = 1.62
are presented in figure 8. Points of transition were measured at each
stagnation pressure from the photographs and the corresponding transition
Reynolds numbers were determined. These transition Reynolds numbers are
shown in figure 9 together with a compilation of data from other sources
which include results for several bodies of revolution, a cone and two
hollow cylinders (refs. 2, 3, 6, 7, and unpublished results). The

ballistic-range results of reference 2 are plotted with ambient pressure
as the abscissa. The wind-tunnel results shown in figure 9 represent
equilibrium temperature conditions. The relative turbulence levels of
the various tunnels are not known, and the possible effects of stagnation
pressure upon these turbulence levels and upon other tunnel conditions
such as Mach number and stream angularities and disturbances, cannot be
determined. In the pressurized ballistic-range tests (ref. 2), any effects
of tunnel turbulence are presumably excluded, although it is possible that
heat-transfer effects and effects of slight oscillations in angle of attack
are present. The results for the bodies of revolution contain effects of
varying pressure gradient over the cylindrical afterbody, and it also
appears that consideration must be given to the length of the adverse pres-
sure gradient as well as to the value of the pressure gradient.

However, in spite of the variety of the test conditions and tech-
niques represented in the summary of data, a definite increase in Reynolds
number for transition with increasing stagnation pressure is evident. The
present results showed an increase with increasing stagnation pressure
ranging from about 3×10^6 at 30 in. Hg to about 5×10^6 at 120 in. Hg.
It is also interesting to note that the results shown for the cone and for
the hollow cylinders which have essentially zero pressure gradient are in
substantial agreement with the results for the bodies of revolution. Up
to the present time, no satisfactory explanation has been found for this
phenomenon, but it is evident that comparisons of wind-tunnel-transition
results or attempts to apply these results to free flight must take into
consideration this phenomenon.

The variation in Reynolds number for transition at the base with Mach
number as determined from schlieren photographs is presented in figure 10
together with a summary of results for cone-cylinder bodies of revolution
(refs. 1, 2, 5, 6, 10, and 12 to 15). The average surface roughness for
these configurations ranges from about 8 to 20 rms microinches. Each
point represents a single value of stagnation pressure; some effect of
stagnation pressure as discussed previously may be seen in the present
results where the low-fineness-ratio bodies have the largest values of
transition Reynolds number. In view of the number of factors which may
influence transition and which may occur as variables in the present com-
pilation, it is not surprising that the results show considerable scatter.
However, it may be seen that, in general, the variation of Reynolds number
for transition with Mach number is to increase with increasing Mach number
and, then, reach a peak in a range of Mach number from about 2.0 to 2.5
and, thereafter, decrease with further increases in Mach number. This
decrease in transition Reynolds number with Mach number is consistent with
theoretical results for the stability of the laminar boundary layer in com-
pressible flow (see, for example, ref. 16). It might be noted that higher
Reynolds numbers for transition have been obtained at the higher Mach num-
bers where boundary-layer cooling was present. For example, a transition

Reynolds number of about 8.5×10^6 has been obtained on a hollow cylinder in the Langley 11-inch hypersonic tunnel at a Mach number of 6.9.

CONCLUDING REMARKS

An investigation of the Reynolds number for transition and the skin-friction drag at zero lift of eight cone-cylinder bodies having varying fineness ratios has been made at Mach numbers of 1.62, 1.93, and 2.41 over a Reynolds number range from 0.3×10^6 to 10×10^6. The accuracy of the skin-friction data was not sufficient to permit any general conclusions to be drawn.

The Reynolds number for transition was indicated to be a function of some parameter which is influenced by changes in stagnation pressure. For the present results, the transition Reynolds number increased with increasing stagnation pressure ranging from about 3×10^6 at 30 in. Hg to about 5×10^6 at 120 in. Hg. Up to the present time, no satisfactory explanation has been found for this phenomenon. Analysis of the present tests results together with the results of other cone-cylinder bodies of revolution having zero-heat transfer showed that the Reynolds number for transition at the base increased with increasing Mach number and reached a peak at a Mach number from about 2.0 to 2.5, and, thereafter, decreased with further increases in Mach number.

Langley Aeronautical Laboratory,
    National Advisory Committee for Aeronautics,
        Langley Field, Va., August 18, 1953.

REFERENCES

1. Potter, J. L.: Friction Drag and Transition Reynolds Number on Bodies
   of Revolution at Supersonic Speeds. NAVORD Rep. 2150, U. S. Naval
   Ord. Lab., White Oak, Md., Aug. 20, 1951.

2. Potter, J. L.: New Experimental Investigations of Friction Drag and
   Boundary Layer Transition on Bodies of Revolution at Supersonic
   Speeds. NAVORD Rep. 2371, U. S. Naval Ord. Lab. (White Oak, Md.),
   Apr. 24, 1952.

3. Jack, John R., and Burgess, Warren C.: Aerodynamics of Slender Bodies
   at Mach Number of 3.12 and Reynolds Numbers From 2×10^6 to 15×10^6.
   I - Body of Revolution With Near-Parabolic Forebody and Cylindrical
   Afterbody. NACA RM E51H13, 1951.

4. Jack, John R., and Gould, Lawrence I.: Aerodynamics of Slender Bodies
   at Mach Number of 3.12 and Reynolds Numbers From 2×10^6 to 15×10^6.
   II. Aerodynamic Load Distributions of Series of Five Bodies Having
   Conical Nose and Cylindrical Afterbodies. NACA RM E52C10, 1952.

5. Jack, John R.: Aerodynamic Characteristics of a Slender Cone-Cylinder
   Body of Revolution at a Mach Number of 3.85. NACA RM E51H17, 1951.

6. Jack, John R.: Aerodynamics of Slender Bodies at Mach Number of 3.12
   and Reynolds Numbers From 2×10^6 to 15×10^6. III - Boundary Layer
   and Force Measurements on a Slender Cone-Cylinder Body of Revolution.
   NACA RM E53B03, 1953.

7. Brinich, Paul F., and Diaconis, Nick S.: Boundary-Layer Development
   and Skin Friction at Mach Number 3.05. NACA TN 2742, 1952.

8. Love, Eugene S., Coletti, Donald E., and Bromm, August F., Jr.: Inves-
   tigation of the Variation With Reynolds Number of the Base, Wave,
   and Skin-Friction Drag of a Parabolic Body of Revolution (NACA RM-10)
   at Mach Numbers of 1.62, 1.93, and 2.41 in the Langley 9-Inch Super-
   sonic Tunnel. NACA RM L52H21, 1952.

9. Love, Eugene S.: The Base Pressure at Supersonic Speeds on Two-
   Dimensional Airfoils and Bodies of Revolution (With and Without Fins)
   Having Turbulent Boundary Layers. NACA RM L53C02, 1953.

10. Love, Eugene S., and O'Donnell, Robert M.: Investigations at Super-
    sonic Speeds of the Base Pressure on Bodies of Revolution With and
    Without Sweptback Stabilizing Fins. NACA RM L52J21a, 1952.

11. Staff of the Computing Section, Center of Analysis (Under Direction
    of Zdeněk Kopal): Tables of Supersonic Flow Around Cones. Tech.
    Rep. No. 1, M.I.T., 1947.

12. Chapman, Dean R.: An Analysis of Base Pressure at Supersonic Veloc-
    ities and Comparison With Experiment. NACA Rep. 1051, 1951.
    (Supersedes NACA TN 2137.)

13. Bogdonoff, Seymour M.: A Preliminary Study of Reynolds Number Effects
    on Base Pressure at M = 2.95. Jour. Aero. Sci., vol. 19, no. 3,
    Mar. 1952, pp. 201-206.

14. Kurzweg, H. H.: Interrelationship Between Boundary Layer and Base
    Pressure. Jour. Aero. Sci., vol. 18, no. 11, Nov. 1951,
    pp. 743-748.

15. Eber, G. R.: Recent Investigation of Temperature Recovery and Heat
    Transmission on Cones and Cylinders in Axial Flow in the N.O.L.
    Aeroballistics Wind Tunnel. Jour. Aero. Sci., vol. 19, no. 1,
    Jan. 1952, pp. 1-6 and 14.

16. Anon.: Bi-Monthly Survey of the Project Hermes. No. 47, Gen. Elec.
    Co., Nov.-Dec. 1949.

45° Bevel to sharp edge

$\frac{1}{4}$"

$\frac{3}{8}$ D

$\frac{7}{8}$"

Strain-gage balance

Sting

Sting support
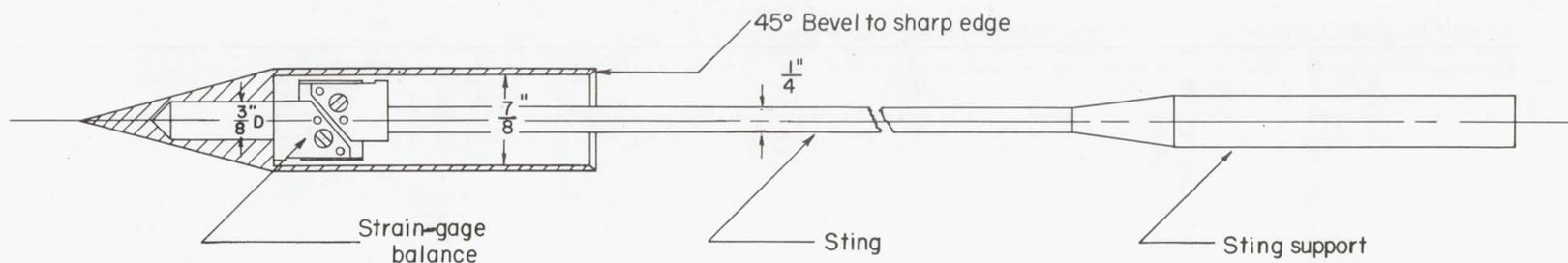
Location of Pressure orifices	
Orifice	y, in
1	0.503
2	0.800
3	1.097
4	1.362
5	1.658

1 2 3 4 5

y

Detail for Models 5—8 only

30°

$\frac{3}{4}$"D $\frac{7}{8}$"D   1"D

$\frac{1}{2}$"

$1\frac{7}{8}$"

Model number 1   2   3   4   5   6   7   8

Model number	Length in inches
1	2
2	3
3	4
4	5
5	6
6	7
7	8
8	9

NACA

Figure 1.- Sketch of models and sting support.
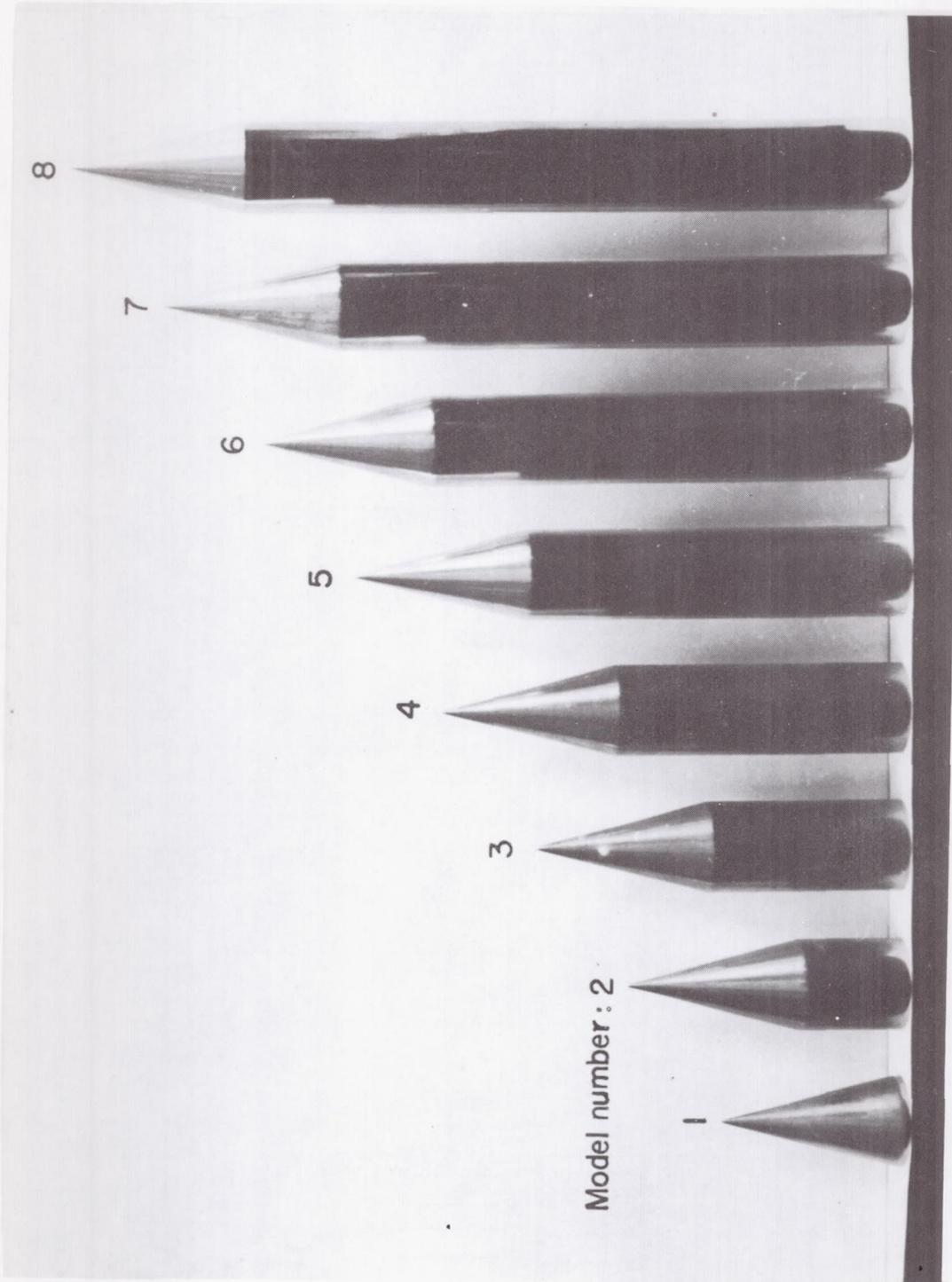
L-80290

Figure 2.- Photograph of models.
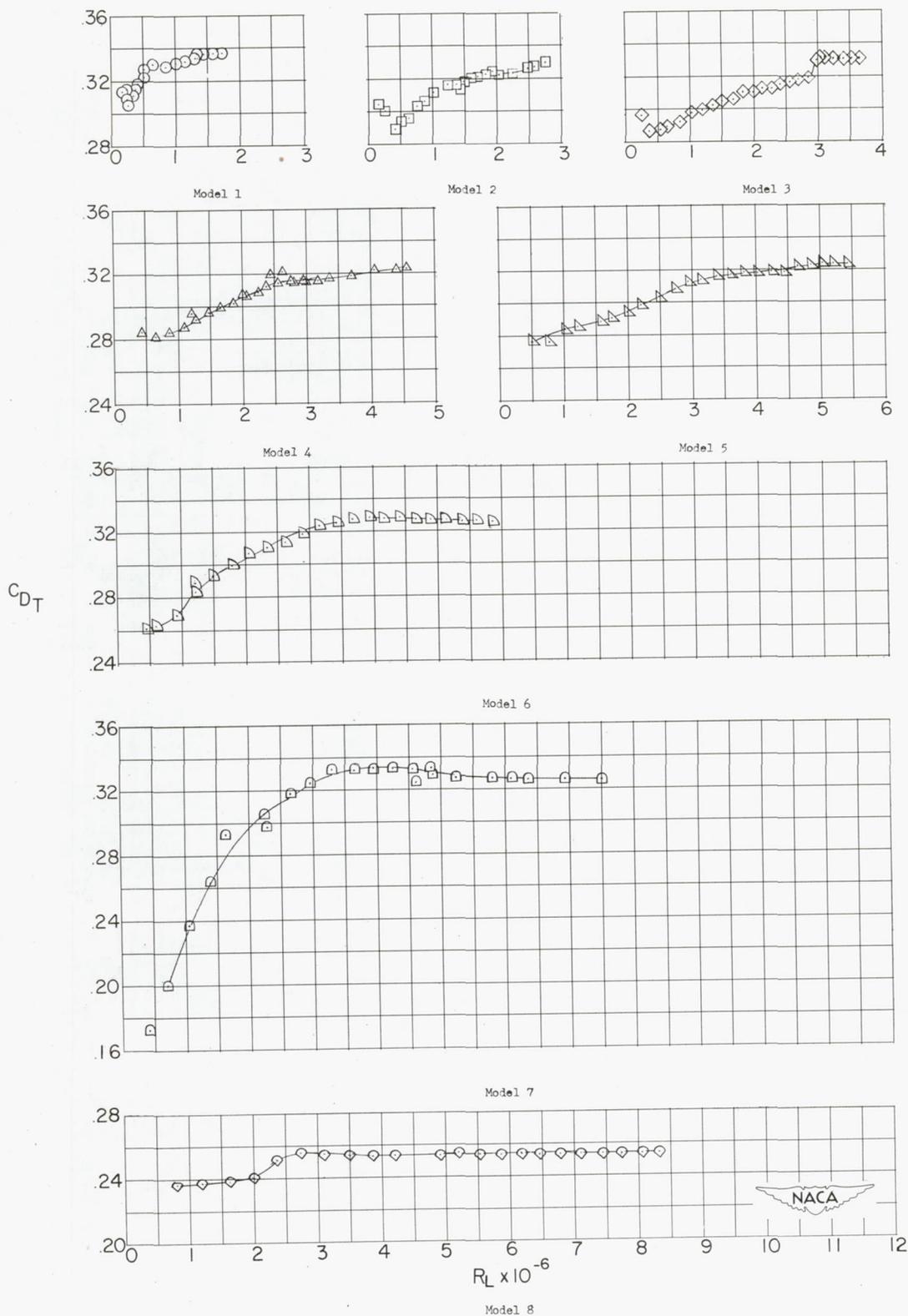
Figure 3.- Variation of total-drag coefficient with Reynolds number
at M = 2.41.
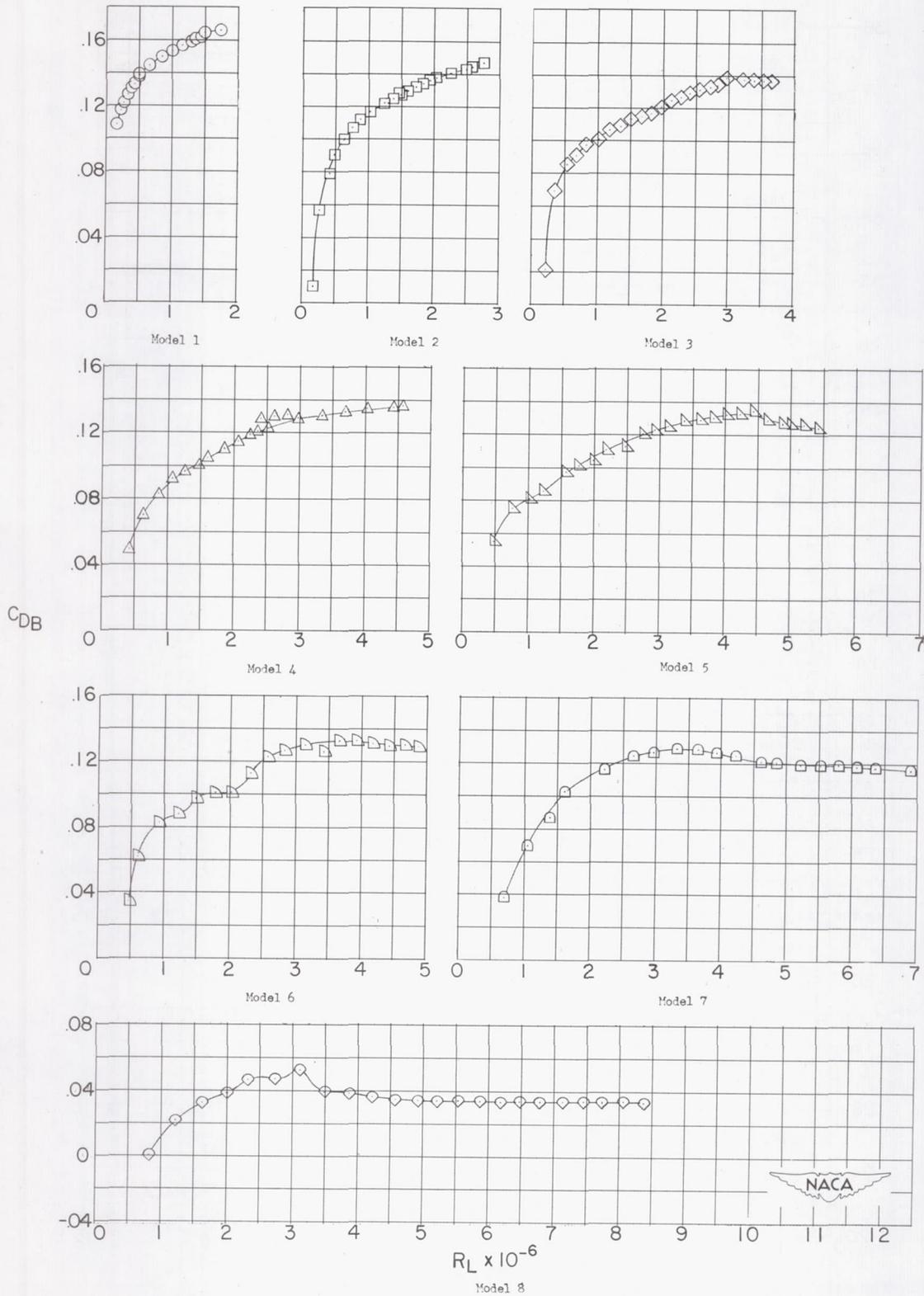
Figure 4.- Variation of base-drag coefficient with Reynolds number
at   M = 2.41.
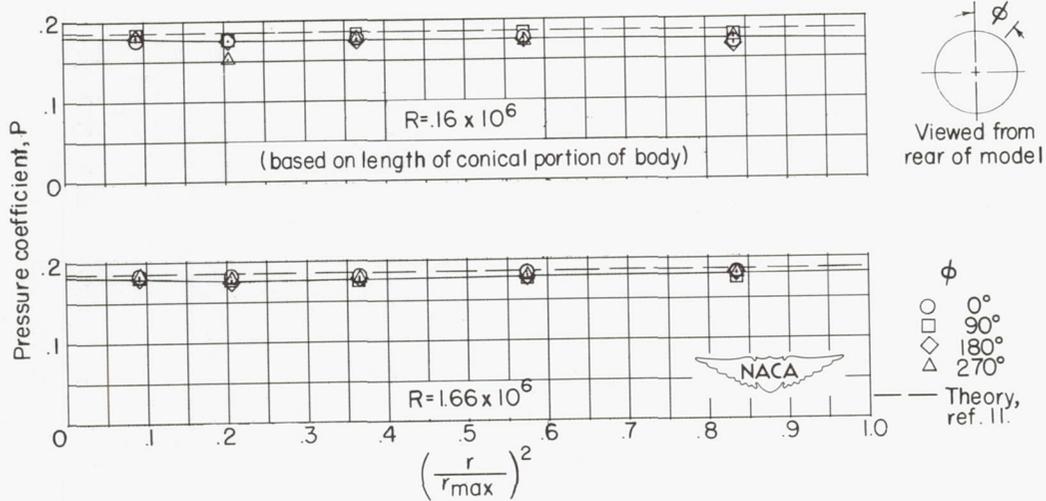
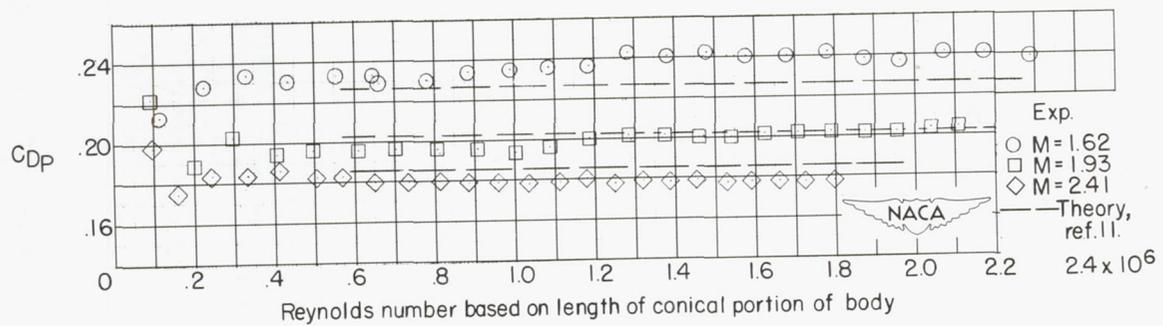Figure 5.- Typical pressure distributions over conical portion of cone-cylinder body. M = 2.41.

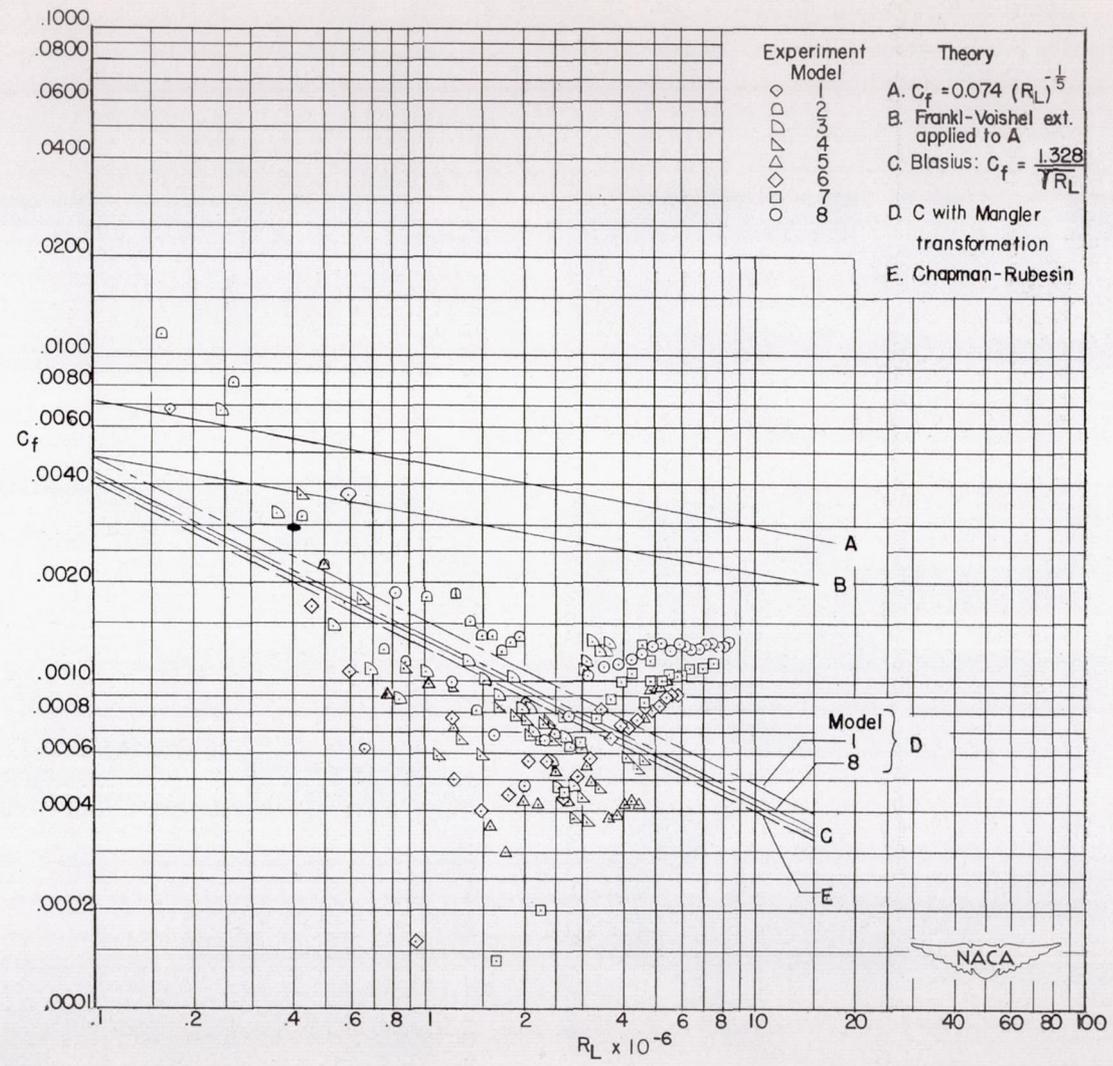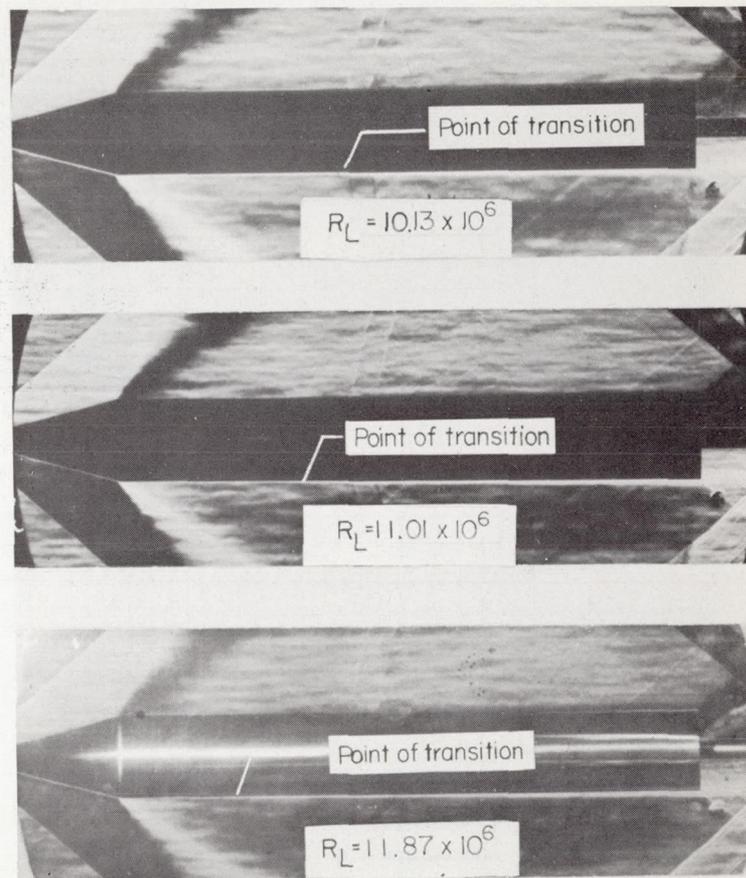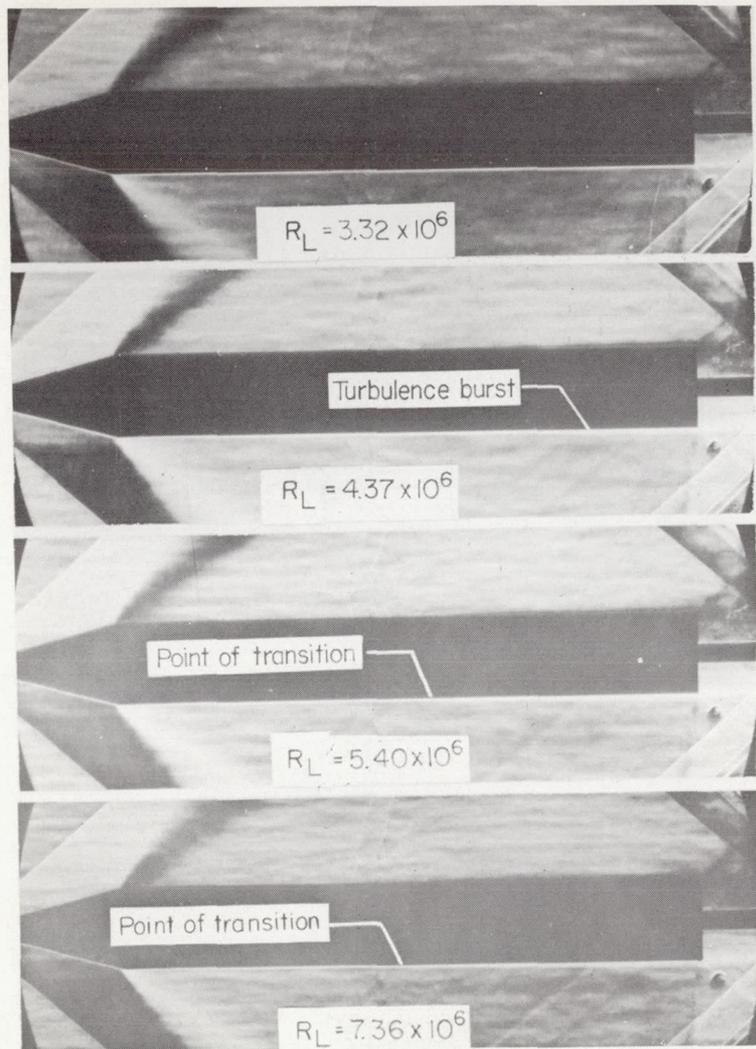Figure 6.- Variation of forebody pressure-drag coefficient with Reynolds number.

Figure 7.- Variation of skin-friction coefficient with Reynolds number
at M = 2.41.

$R_L = 3.32 \times 10^6$

Turbulence burst

$R_L = 4.37 \times 10^6$

Point of transition

$R_L = 5.40 \times 10^6$

Point of transition

$R_L = 7.36 \times 10^6$

Point of transition

$R_L = 10.13 \times 10^6$

Point of transition

$R_L = 11.01 \times 10^6$

Point of transition

$R_L = 11.87 \times 10^6$

L-80291

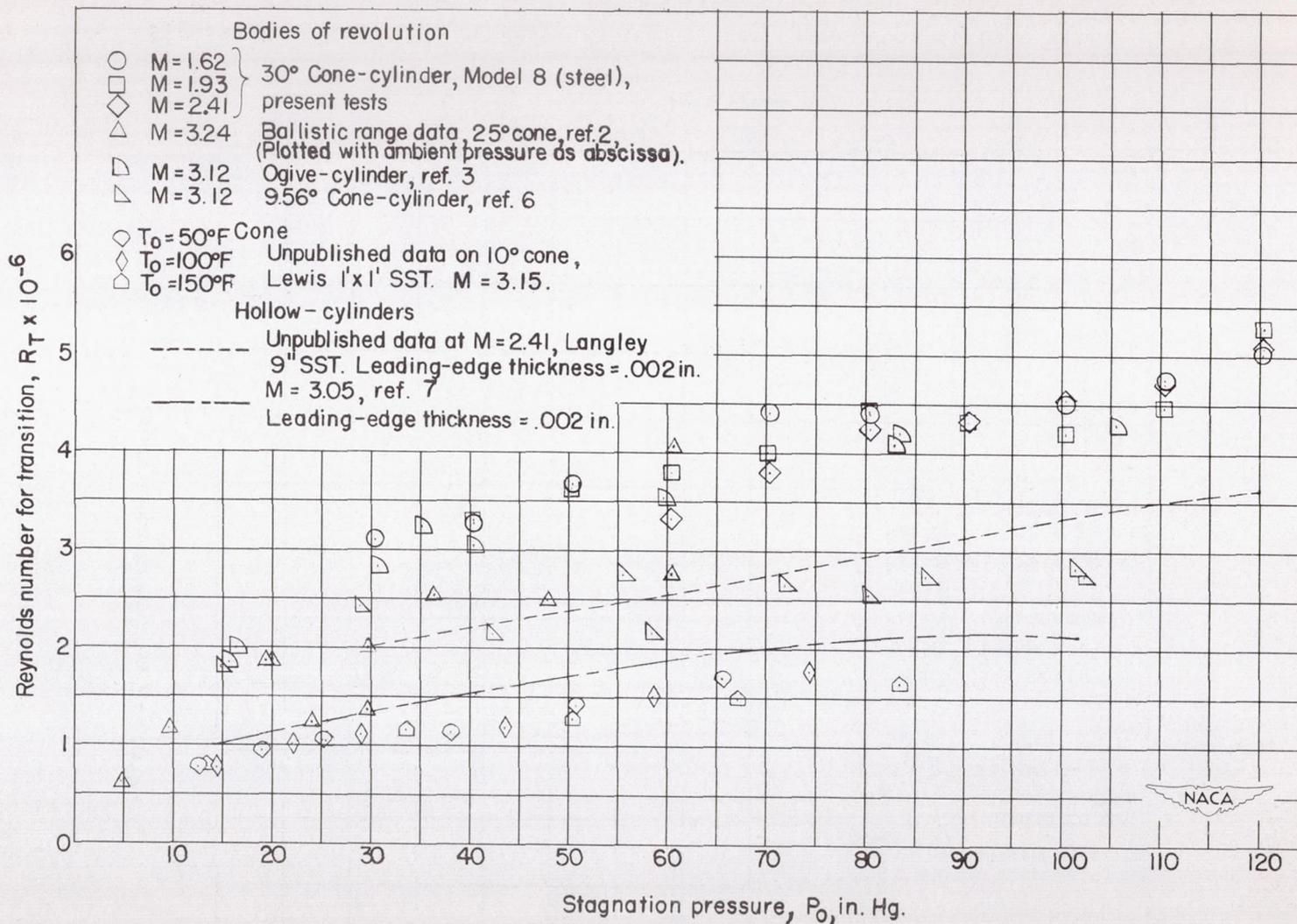Figure 8.- Schlieren photographs of model 8 for various Reynolds numbers
at M = 1.62.

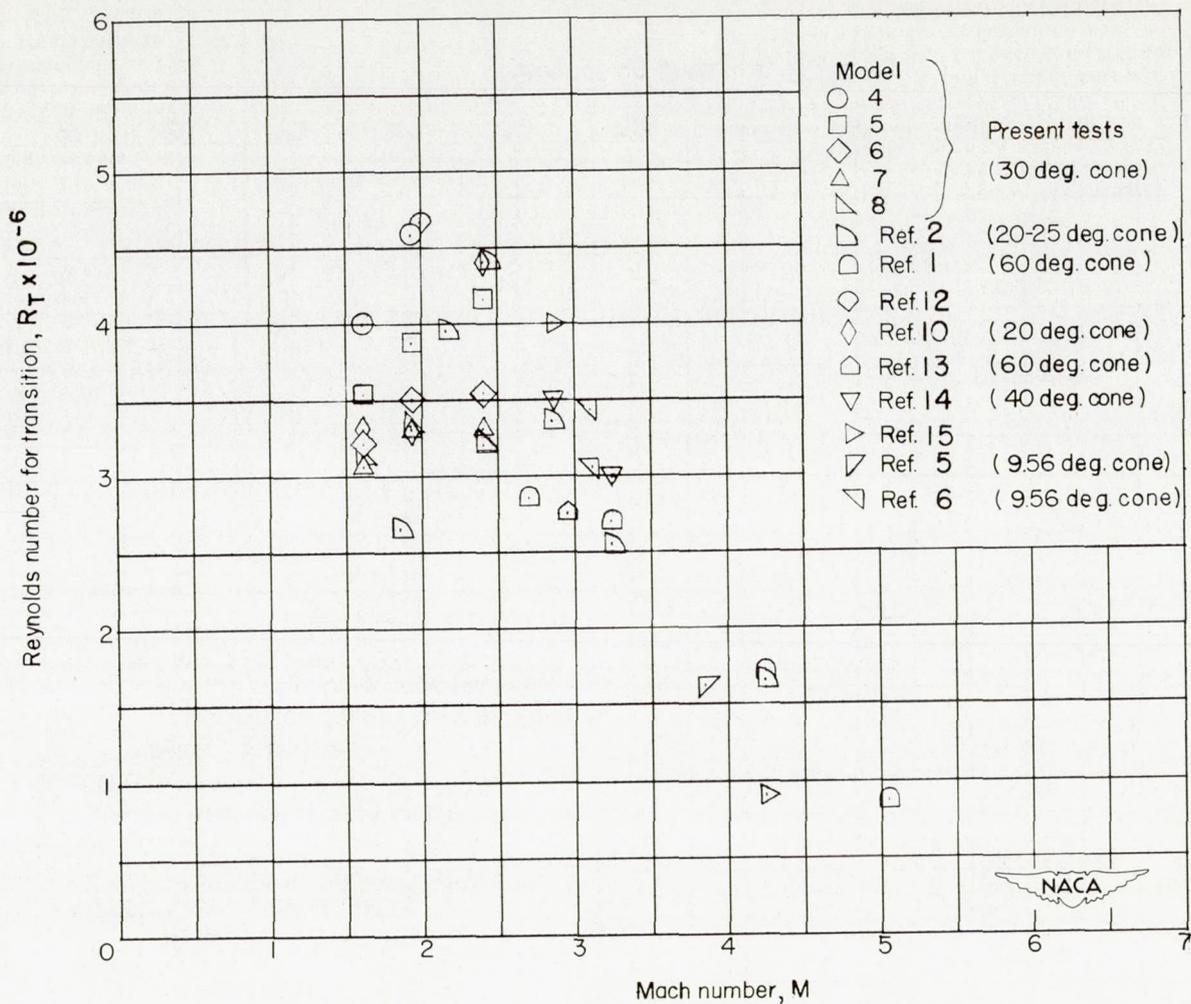Figure 9.- Variation of Reynolds number for transition with stagnation pressure.

Figure 10.- Variation of Reynolds number for transition at base with
Mach number. Summary of available results for cone-cylinder bodies
of revolution; zero heat transfer.